

ARTICLE

Open Access

# m<sup>6</sup>A-mediated ZNF750 repression facilitates nasopharyngeal carcinoma progression

Panpan Zhang<sup>1</sup>, Qiuping He<sup>2</sup>, Yuan Lei<sup>1</sup>, Yingqin Li<sup>1</sup>, Xin Wen<sup>1</sup>, Mengzhi Hong<sup>2</sup>, Jian Zhang<sup>1</sup>, Xianyue Ren<sup>3</sup>, Yaqin Wang<sup>1</sup>, Xiaojing Yang<sup>1</sup>, Qingmei He<sup>1</sup>, Jun Ma<sup>1</sup> and Na Liu<sup>1</sup>

## Abstract

Nasopharyngeal carcinoma (NPC) progression is regulated by genetic, epigenetic, and epitranscript modulation. As one of the epitranscript modifications, the role of N6-Methyladenosine (m<sup>6</sup>A) has not been elucidated in NPC. In the present study, we found that the poorly methylated gene *ZNF750* (encoding zinc finger protein 750) was downregulated in NPC tumor tissues and cell lines. Ectopic expression of *ZNF750* blocked NPC growth in vitro and in vivo. Further studies revealed that m<sup>6</sup>A modifications maintained the low expression level of *ZNF750* in NPC. Chromatin immunoprecipitation sequencing identified that *ZNF750* directly regulated *FGF14* (encoding fibroblast growth factor 14), ablation of which reversed *ZNF750*'s tumor repressor effect. Moreover, the *ZNF750*-*FGF14* signaling axis inhibited NPC growth by promoting cell apoptosis. These findings uncovered the critical role of m<sup>6</sup>A in NPC, and stressed the regulatory function of the *ZNF750*-*FGF14* signaling axis in modulating NPC progression, which provides theoretical guidance for the clinical treatment of NPC.

## Introduction

Nasopharyngeal carcinoma (NPC) is a malignant head and neck cancer with apparent regional aggregation<sup>1–3</sup>. With the advancement of intensity-modulated radiation therapy and combined chemotherapy, great progress has been made in local and regional control of NPC. However, there are still about 30% of patients with NPC develop distant metastasis and/or recurrence<sup>4</sup>. Revealing the underlying mechanism governing NPC progression would identify novel targets to develop clinical treatment strategies.

Our previous genome-wide methylation profiling study revealed the methylation status between 24 NPC tissues and 24 normal nasopharyngeal epithelial tissues, from which a list of hypermethylated and hypomethylated genes was composed (GSE52068)<sup>5</sup>. Zinc Finger Protein 750 (*ZNF750*), as a transcription factor belonging to one of the Zinc Finger Protein family members, was the top-ranked hypomethylated gene in the dataset. Previous findings revealed that *ZNF750* serves as a tumor repressor in oral squamous cell carcinoma<sup>6</sup> and esophageal squamous cell carcinoma<sup>7</sup>. However, the mechanism by *ZNF750* governs tumorigenesis and the role of *ZNF750* in NPC remain largely unknown.

N<sup>6</sup>-methyladenosine (m<sup>6</sup>A) is the most common mRNA internal modification in eukaryotic organisms<sup>8–10</sup>. m<sup>6</sup>A mRNA methylation is catalyzed by multicomponent methyltransferases, among which methyltransferase like 3 (*METTL3*) and *METTL14* have been characterized<sup>11,12</sup>. The methylated mRNA is recognized by protein “readers” YTH N6-methyladenosine RNA binding protein 1–3

Correspondence: Na Liu (liun1@sysucc.org.cn)

<sup>1</sup>State Key Laboratory of Oncology in South China, Collaborative Innovation Centre of Cancer Medicine, Guangdong Key Laboratory of Nasopharyngeal Carcinoma Diagnosis and Therapy, Sun Yat-sen University Cancer Center, 510060 Guangzhou, China

<sup>2</sup>Zhongshan School of Medicine, Sun Yat-sen University, 510080 Guangzhou, China

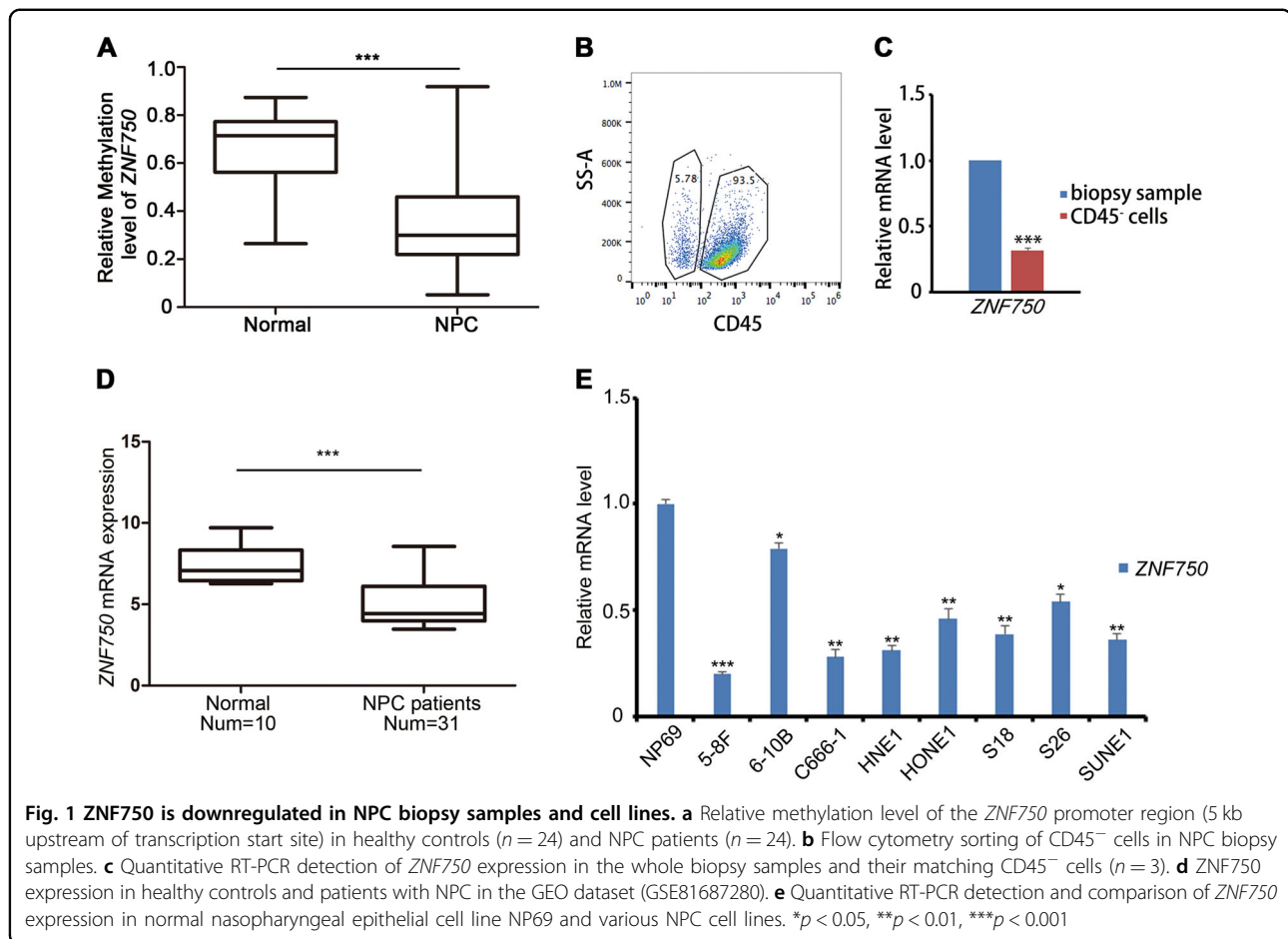
Full list of author information is available at the end of the article.

These authors contributed equally: Panpan Zhang, Qiuping He, Yuan Lei. Edited by M. Agostini.

© The Author(s) 2018



**Open Access** This article is licensed under a Creative Commons Attribution 4.0 International License, which permits use, sharing, adaptation, distribution and reproduction in any medium or format, as long as you give appropriate credit to the original author(s) and the source, provide a link to the Creative Commons license, and indicate if changes were made. The images or other third party material in this article are included in the article's Creative Commons license, unless indicated otherwise in a credit line to the material. If material is not included in the article's Creative Commons license and your intended use is not permitted by statutory regulation or exceeds the permitted use, you will need to obtain permission directly from the copyright holder. To view a copy of this license, visit <http://creativecommons.org/licenses/by/4.0/>.



(YTHDF1–3)<sup>9,13</sup>, which regulate mRNA stability and localization in the cell<sup>14</sup>. The importance of m<sup>6</sup>A modification in cancer progression is only beginning to emerge. Previous studies showed that AlkB homolog 5 (ALKBH5), as the RNA demethylase of m<sup>6</sup>A, mediates the promotion of breast cancer stem cell phenotype by elevating NANOG expression in the hypoxic environment<sup>15</sup>. Moreover, in acute myeloid leukemia (AML) cells, METTL3 was abundantly expressed and promoted *MYC*, *BCL2*, and *PTEN* translation through m<sup>6</sup>A modification, which inhibited cell differentiation and fueled leukemia progression<sup>16</sup>. However, the possible function of m<sup>6</sup>A in NPC is still completely unknown.

In this study, we identified that *ZNF750*, as a hypomethylated gene, was downregulated in NPC tumor tissues and cell lines. Overexpression of *ZNF750* inhibited the growth of NPC cells in vitro and in vivo. An m<sup>6</sup>A RNA immunoprecipitation (RIP) assay revealed that m<sup>6</sup>A was enriched in the *ZNF750* coding sequence (CDS) and contributed to *ZNF750*'s low expression in NPC. Moreover, chromatin immunoprecipitation sequencing (ChIP-Seq) identified fibroblast growth factor 14 (FGF14) as the downstream target of *ZNF750*, and blocking FGF14

reversed the tumor repressor effect of *ZNF750* in NPC cells. These findings revealed the essential regulatory role of the *ZNF750*-FGF14 signaling axis and highlighted the importance of m<sup>6</sup>A modification in modulating gene expression post-transcriptionally in NPC.

## Results

### *ZNF750* is downregulated in NPC biopsy samples and cell lines

Despite previous findings indicating that *ZNF750* is frequently mutated in head and neck squamous cell carcinoma (HNSC)<sup>17,18</sup> and esophageal carcinoma (ESCA)<sup>19</sup>, *ZNF750* was not mutated in the majority of HNSC patients in the cBioPortal dataset<sup>20,21</sup> (Figure S1A, B). In our previous NPC methylation dataset (GSE52068), *ZNF750* was identified as hypomethylated (Fig. 1a). However, the mRNA expression level of *ZNF750* did not seem to be correlated with its methylation status in HNSC (Figure S1B). To identify the expression level of *ZNF750* in NPC tissue samples,  $CD45^+$  cells were sorted to avoid the contamination from lymphocyte cells (Fig. 1b). *ZNF750* expression was decreased in  $CD45^+$  cells in NPC samples ( $n = 25$ ) (Fig. 1c). In The Cancer Genome Atlas

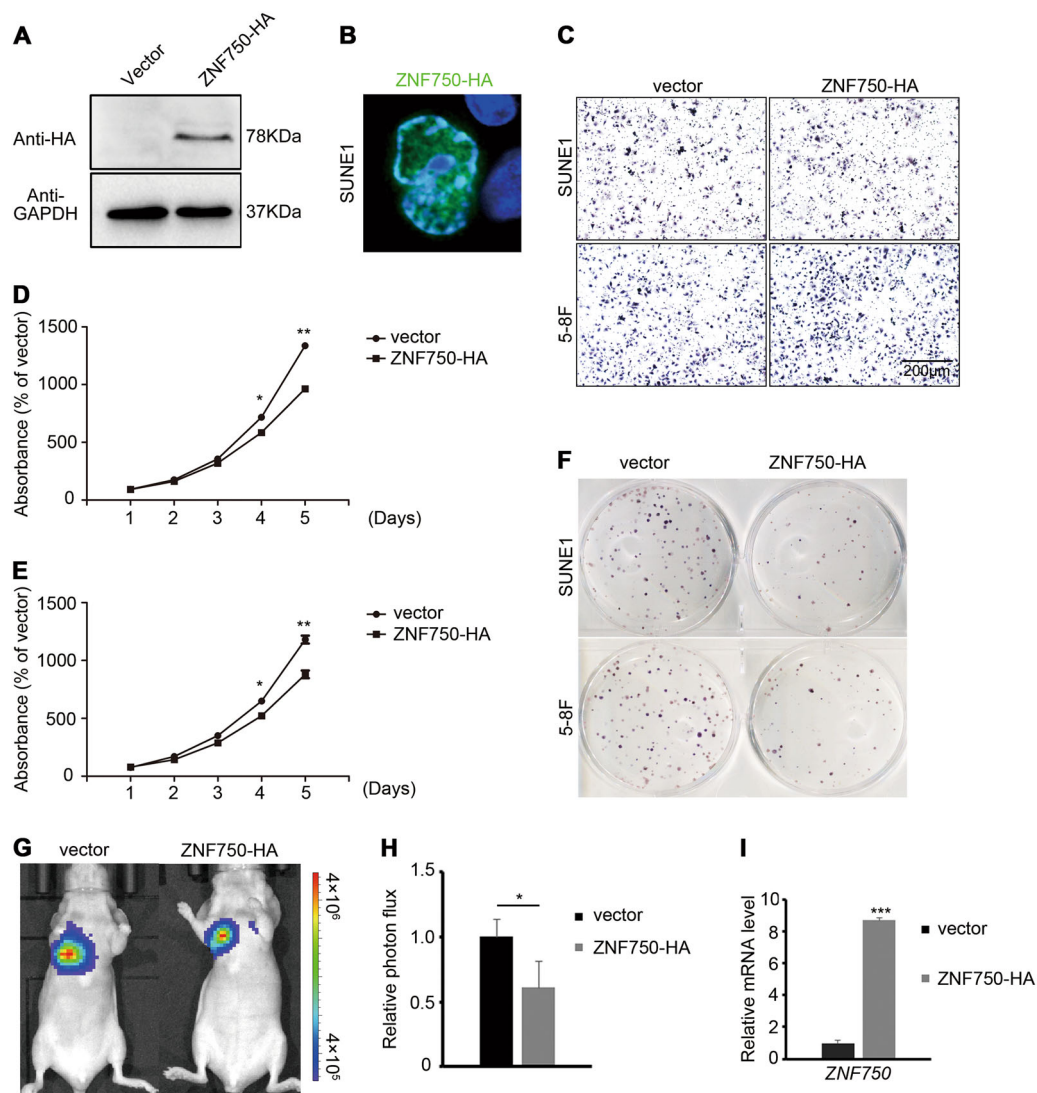
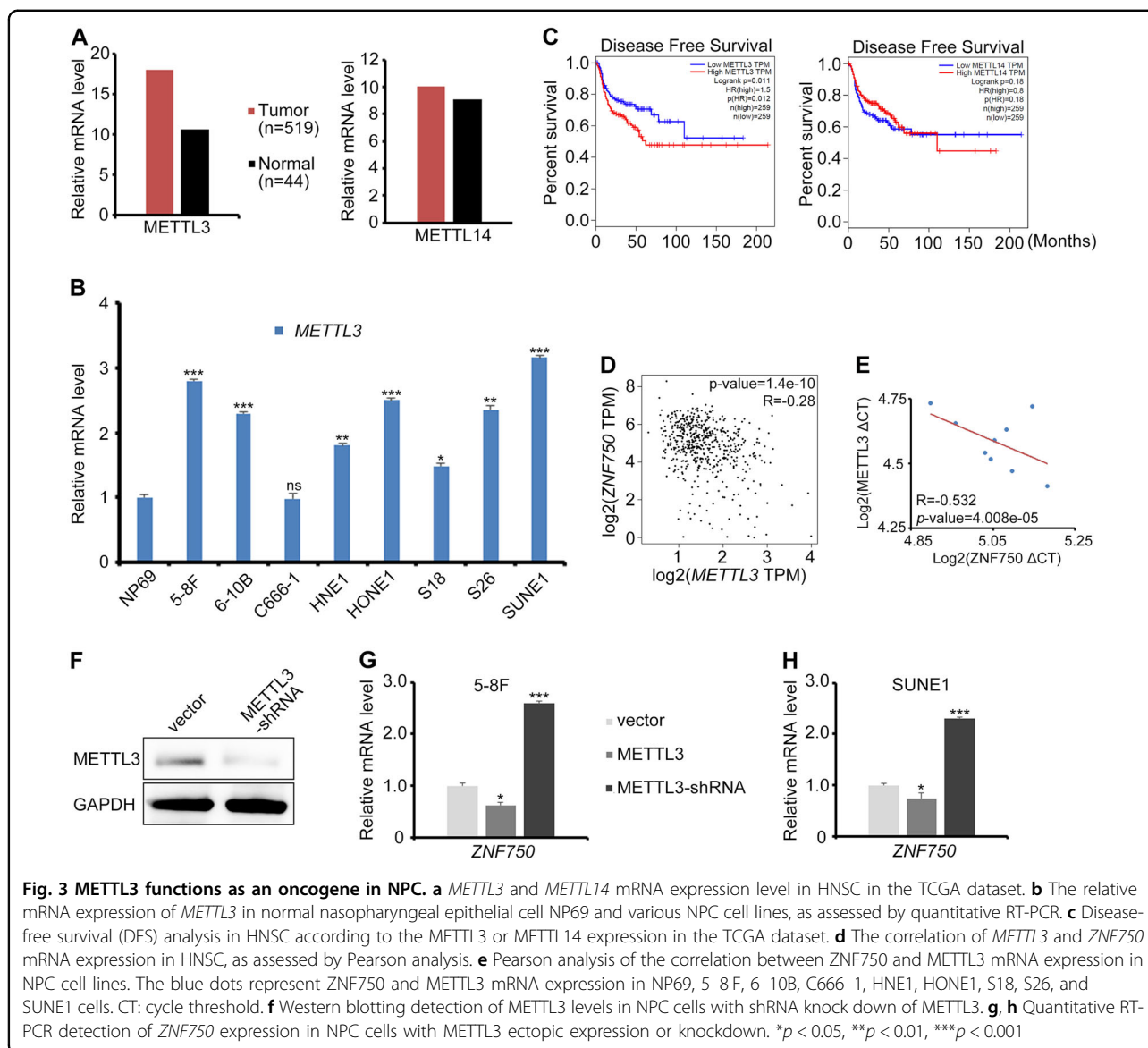


**Fig. 2** ZNF750 represses NPC growth in vitro and in vivo. **a** Western blotting detection of ZNF750-HA expression in SUNE1 cells. **b** Immunofluorescence detection of HA staining in SUNE1 cells with ZNF750-HA overexpression. **c** Transwell assay of SUNE1 and 5–8 F cells with or without ZNF750-HA ectopic expression. **d, e** CCK-8 assay of SUNE1 and 5–8 F cells with or without ZNF750-HA ectopic expression. **f** Colony formation assay of NPC cells with and without ZNF750-HA ectopic expression. **g, h** Tumor cell absorbance intensity and the quantification analysis of vector ( $n = 5$ ) and ZNF750 overexpressed ( $n = 6$ ) groups 2 weeks after tumor cell implantation in mice. **i** The mRNA expression level of ZNF750 in xenograft tumors. \* $p < 0.05$ , \*\* $p < 0.01$

(TCGA) dataset, ZNF750 expression was significantly downregulated in ESCA, HNSC, and skin cutaneous melanoma (SKCM) (Figure S1C). We then compared ZNF750 mRNA expression levels between normal nasopharynx and NPC tissue samples using the Gene Expression Omnibus (GEO) dataset. Compared with that in normal tissues, the expression of ZNF750 was significantly downregulated in NPC tissue samples (Fig. 1d). Moreover, in NPC cell lines, ZNF750 expression was also significantly decreased (Fig. 1e). These results suggested that the expression of ZNF750 was frequently downregulated in NPC, regardless of its methylation status.

### ZNF750 represses NPC growth in vitro and in vivo

To study the function of ZNF750 in NPC, we firstly overexpressed ZNF750 in NPC cells (Fig. 2a). We observed that ZNF750 was localized in cell nucleus (Fig. 2b), indicative of its transcriptional regulatory role in NPC cells. We then detected the NPC cell invasive and proliferative abilities of SUNE1 and 5–8 F that overexpressed ZNF750. The results showed that the invasive ability of NPC cells were not affected, while cell growth and colony formation was reduced significantly (Fig. 2c–f). To test the tumor repressor role of ZNF750 in vivo, SUNE1 cells with luciferase



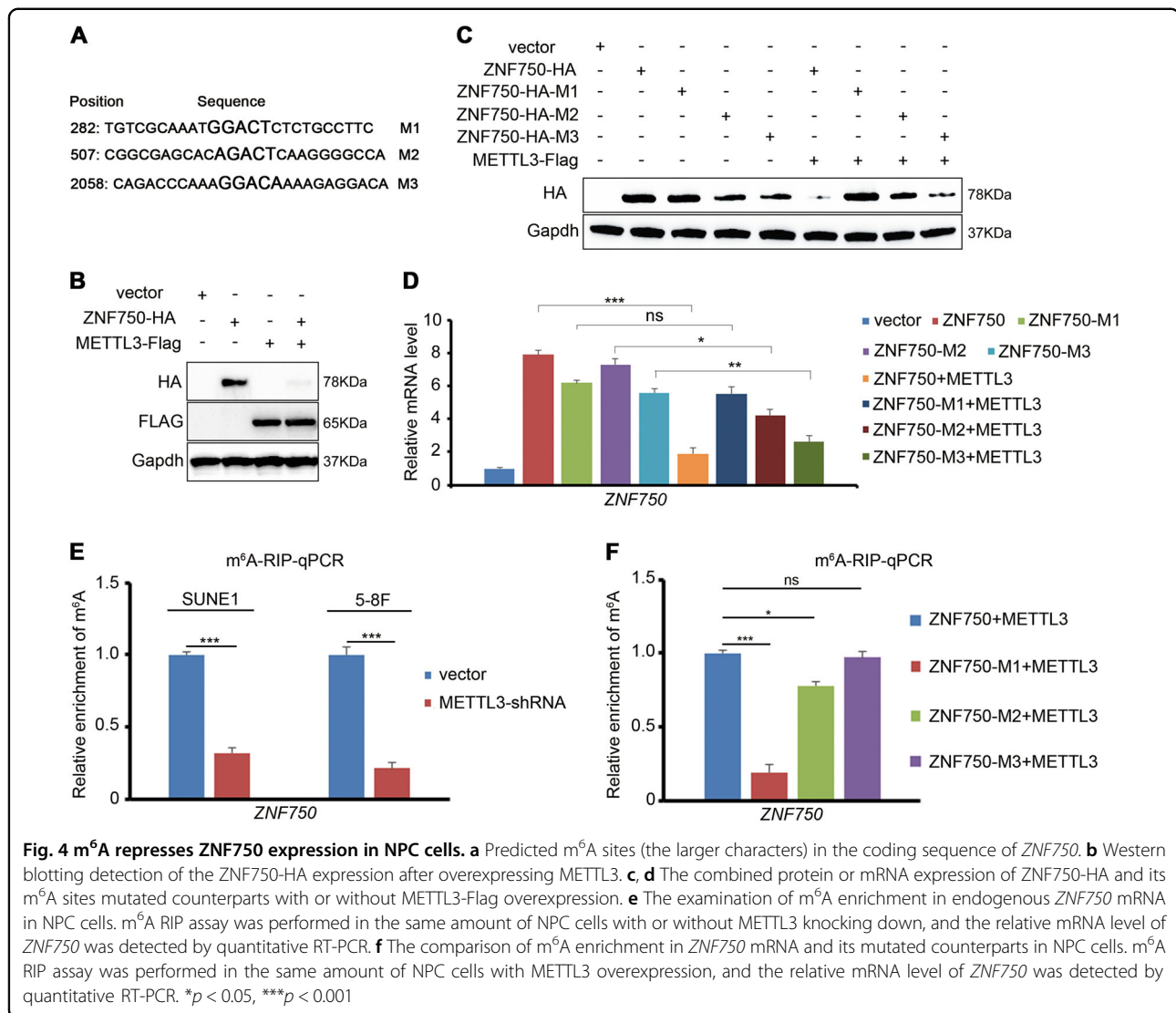
activity were subcutaneously injected into nude mice. We found that ectopic expression of *ZNF750* blocked tumor cell growth (Fig. 2g–i). Moreover, the HNSC patients with higher expression levels of *ZNF750* displayed better disease-free survival (DFS) compared with those with low *ZNF750* levels (Figure S1D). These results revealed that *ZNF750* acts as a tumor repressor in NPC.

#### m<sup>6</sup>A maintains the mRNA stability of *ZNF750* in NPC cells

In our previous NPC methylation dataset (GSE52068), *ZNF750* was listed as the top hypomethylated gene in NPC patients (Supplementary Table 1). Considering the low mRNA expression level of *ZNF750* in NPC, we wondered whether there is a post-transcriptional

modification governing the mRNA stability of *ZNF750*. The methyltransferases *METTL3* or *METTL14* were responsible for modulating mRNA stability post-transcriptionally. However, only *METTL3* displayed an apparent increase in HNSC tissues and NPC cell lines (Fig. 3a, b), and the high expression level of *METTL3* correlated with poor DFS in HNSC patients (Fig. 3c). Moreover, the *METTL3* expression level was negatively correlated with the *ZNF750* expression level in HNSC to some extent (Fig. 3d), and in NPC cell lines (Fig. 3e). Knocking down *METTL3* stimulated endogenous *ZNF750* expression, and vice versa (Fig. 3f–h).

The online tool SRAMP predicted three m<sup>6</sup>A recognition sites with high confidence in the coding sequence

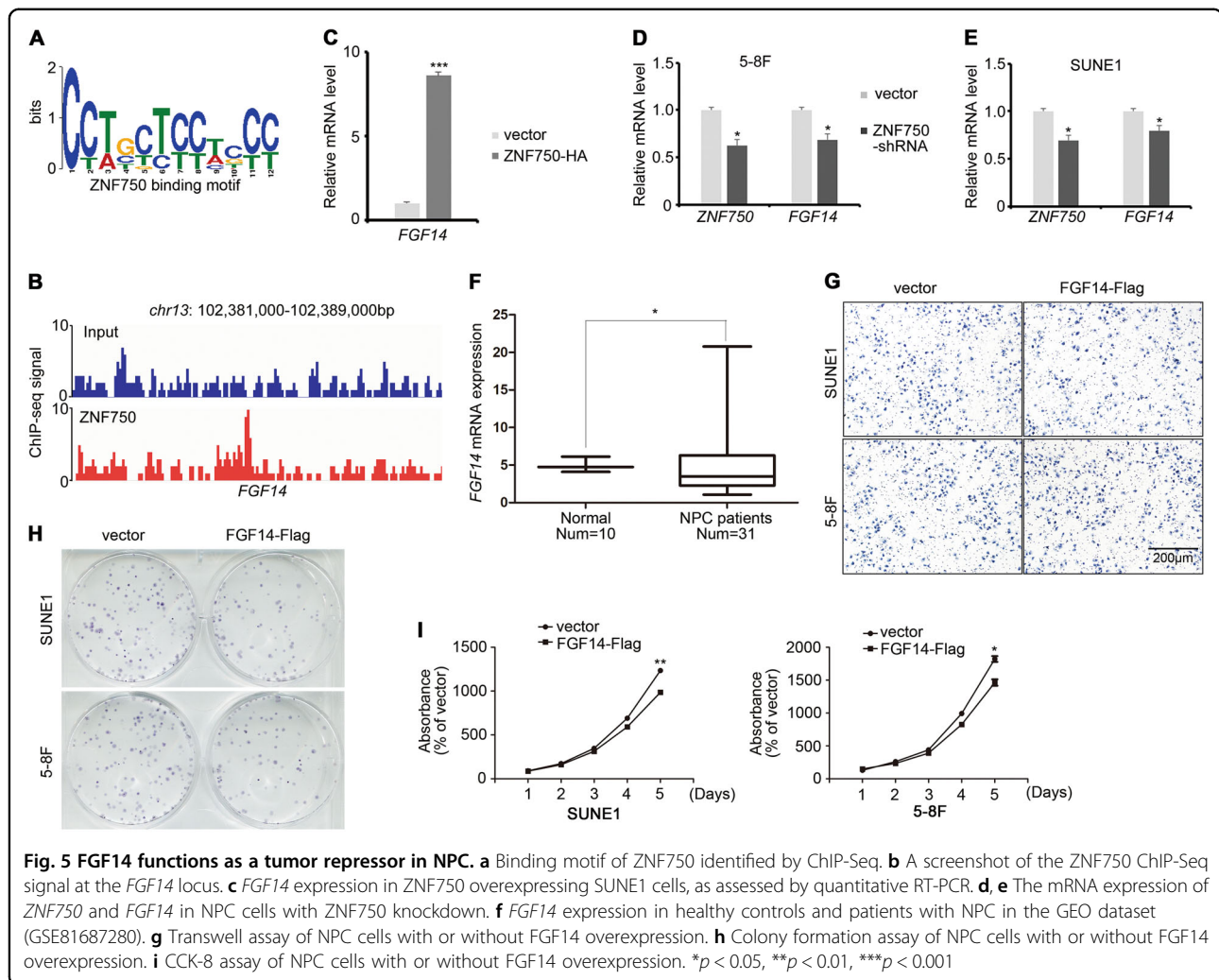


(CDS) of ZNF750 (Fig. 4a). To confirm whether the m<sup>6</sup>A modification is applied to RNA after transcription, we overexpressed METTL3 in NPC cells. The western blotting results showed that ZNF750 expression level was dramatically reduced (Fig. 4b). Then, the three m<sup>6</sup>A recognition sites in the ZNF750 CDS region were mutated respectively (GAC to GCC). Upon METTL3 overexpression, both the ZNF750-M2 and ZNF750-M3 displayed an apparent decrease (Fig. 4c, d), indicating that m<sup>6</sup>A modulated ZNF750 expression mainly through the M1 region in NPC cells, despite the fact that M2 and M3 might also be recognized to some extent. To confirm the existence of the m<sup>6</sup>A modification in the ZNF750 CDS directly, an m<sup>6</sup>A RIP assay in NPC cells was performed. Compared with its counterpart control, m<sup>6</sup>A enrichment in ZNF750 was significantly decreased upon METTL3 knockdown (Fig. 4e), supporting the

view that ZNF750 mRNA possessed METTL3-dependent m<sup>6</sup>A modifications. Moreover, consistent with the results shown in Fig. 3c, most of the m<sup>6</sup>A was found to be enriched in the M1 region of ZNF750 (Fig. 4f). These results demonstrated that m<sup>6</sup>A maintained the mRNA stability of ZNF750 in NPC cells.

#### ZNF750 functions through modulating FGF14 expression

We next addressed the functional mechanism of ZNF750 in repressing NPC growth. ChIP-Seq against ZNF750 was performed to explore its downstream targets (Fig. 5a), among which FGF14 was found to be highly enriched (Fig. 5b, Supplementary Table 2). Quantitative RT-PCR confirmed that FGF14 was upregulated upon ZNF750 overexpression (Fig. 5c), and was downregulated upon ZNF750 knockdown (Fig. 5d, e). Moreover, the expression of FGF14 was also decreased in patients with



NPC (Fig. 5f). To identify the role of FGF14 in NPC, we detected the invasive and proliferative ability of NPC cells overexpressing *FGF14*. The results showed that FGF14 did not influence cell invasion (Fig. 5g). However, the growth and colony formation abilities of NPC cells were significantly reduced (Fig. 5h, i), supporting the view that FGF14 acts as a tumor repressor in NPC.

To further confirm whether FGF14 functions as direct downstream of ZNF750, we mutated the binding site of ZNF750 in the promoter of *FGF14* (43 base pair upstream of transcription start site) (Fig. 6a). A luciferase reporter assay was performed, which showed that ZNF750 directly regulated the expression of *FGF14* in NPC cells (Fig. 6b). We then asked whether inhibiting FGF14 would reverse the tumor repressor function of ZNF750 in vitro and in vivo. After overexpressing ZNF750 and blocking *FGF14* expression simultaneously in NPC cells, we found that *FGF14* knockdown promoted the growth of NPC cells that overexpressed ZNF750 (Fig. 6c–f). Moreover, the inhibition of NPC tumor

growth in mice after *ZNF750* overexpression was reversed by *FGF14* knockdown (Fig. 6g–j). These data confirmed that FGF14 functions directly downstream of ZNF750 in NPC.

#### The ZNF750-FGF14 signaling axis accelerates NPC cell apoptosis

We next asked how the ZNF750-FGF14 signaling axis inhibited NPC cell growth. We firstly examined the cell cycle status of NPC cells with *ZNF750* or *FGF14* overexpression after 5-ethynyl-2'-deoxyuridine (EdU) incorporation, which showed that ZNF750 or FGF14 did not alter the cell cycle status (Fig. 7a, b). In xenograft tumors, Ki67 staining did not change significantly after *ZNF750* overexpression (Fig. 7c), indicating the proliferation capacity was unaffected. Then we examined whether cell apoptosis accounted for the impaired cell growth upon *ZNF750* or *FGF14* overexpression. Annexin V and PI staining revealed that both ZNF750 and FGF14 promoted NPC cell apoptosis (Fig. 7d, e). Moreover,

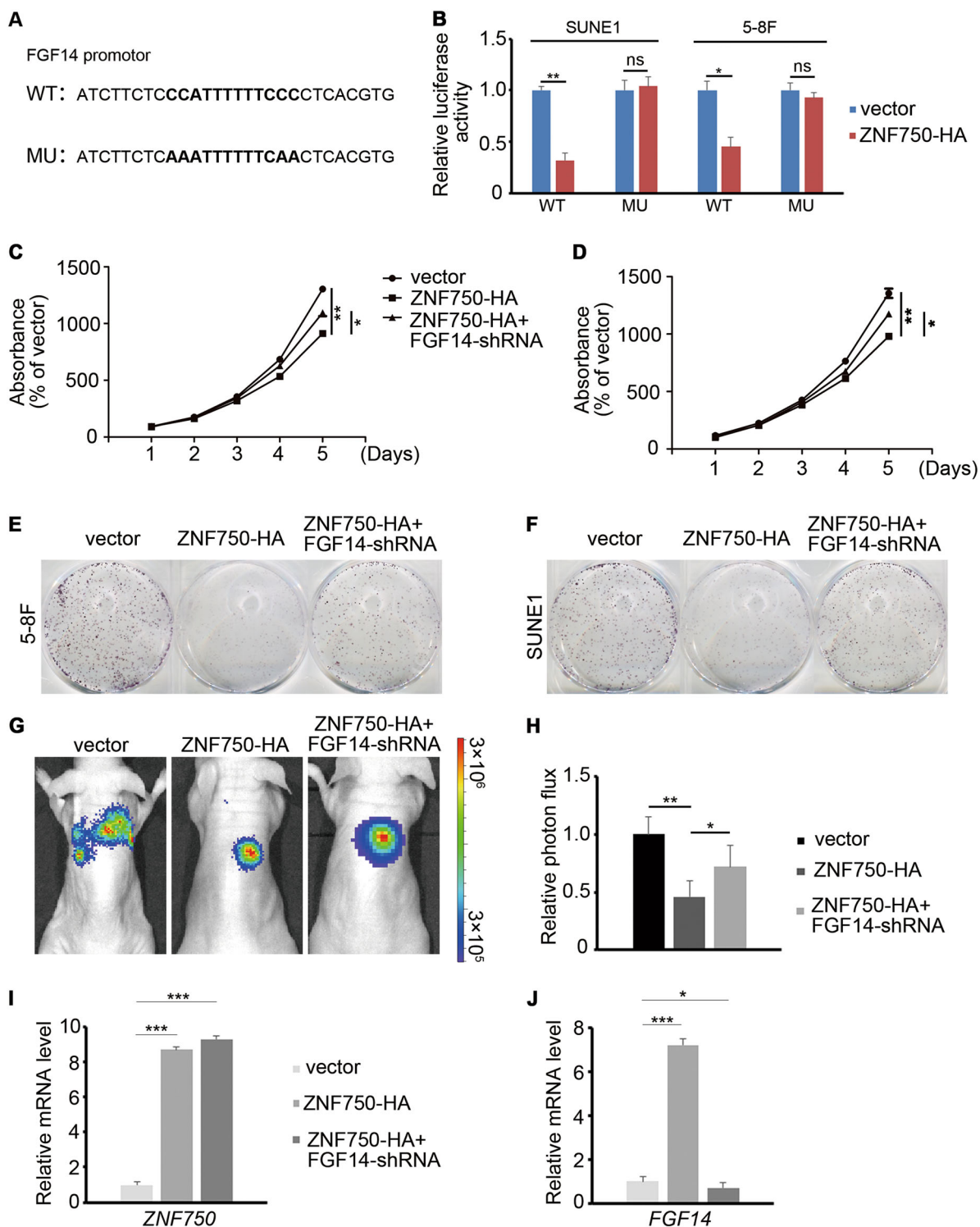
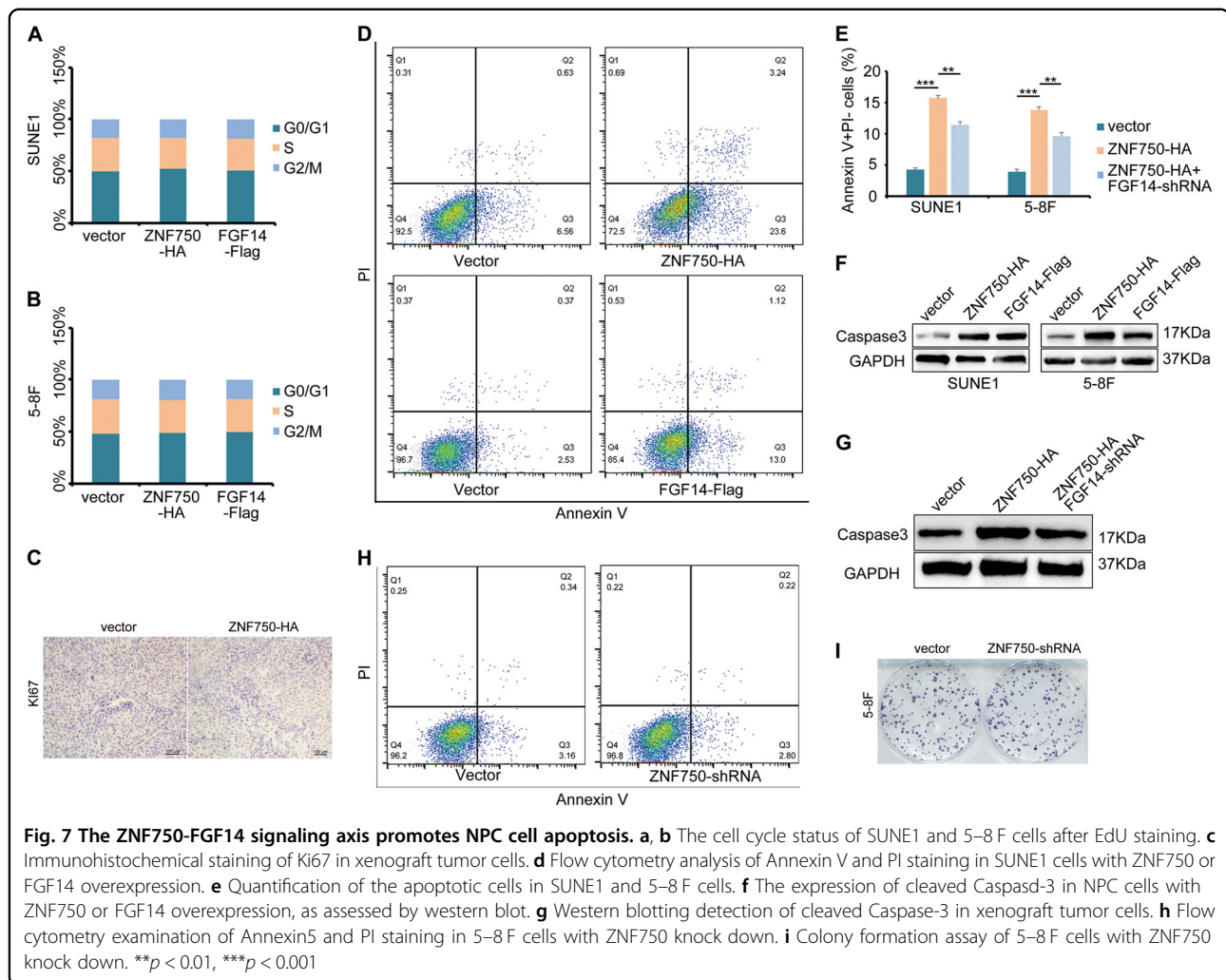


**Fig. 6** *FGF14* serves as the downstream target of *ZNF750*. **a** *ZNF750* binding site with and without mutation in the promoter of *FGF14*. **b** Luciferase activity of *FGF14* wild-type or mutated NPC cells with or without *ZNF750* overexpression. **c, d** CCK-8 assay of NPC cells with *ZNF750* overexpression or *FGF14* knockdown. **e, f** Colony formation assay of NPC cells with *ZNF750* overexpression or *FGF14* knockdown. **g, h** Tumor cell absorbance intensity and the quantification analysis of vector ( $n = 5$ ), *ZNF750* overexpression ( $n = 5$ ), and *ZNF750* overexpression combined with *FGF14* knockdown groups two weeks after tumor cell implantation in mice. **i, j** Quantitative RT-PCR detection of *ZNF750* and *FGF14* expression in xenograft tumor cells. \* $p < 0.05$ , \*\* $p < 0.01$ , \*\*\* $p < 0.001$



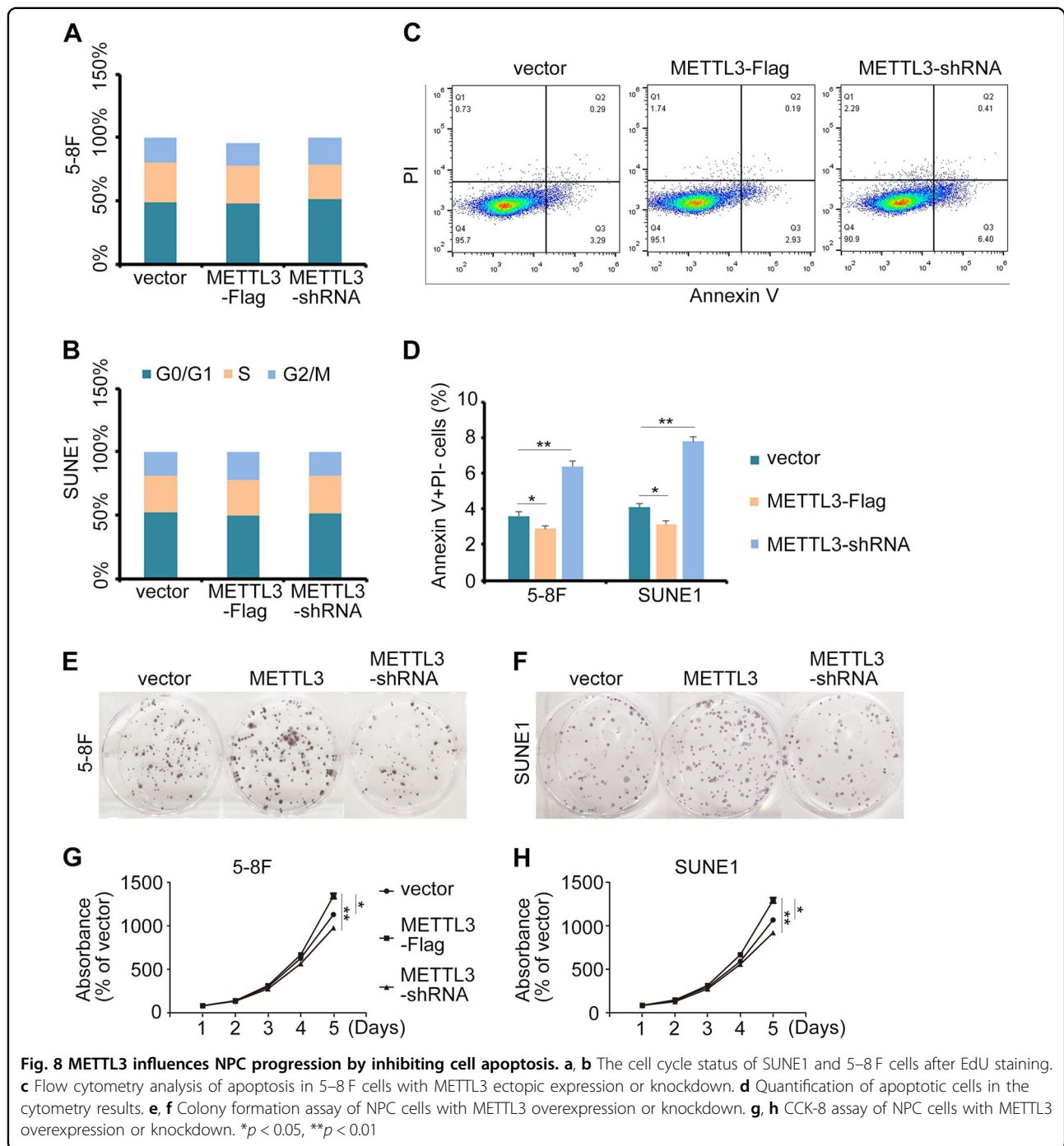
knocking down FGF14 partially decreased the proportion of apoptotic cells, suggesting that ZNF750's regulation of NPC cell apoptosis was dependent on FGF14 expression. Furthermore, the expression of cleaved Caspase-3 was also elevated in NPC cell lines and xenograft tumors (Fig. 7f, g), confirming that the ZNF750-FGF14 axis repressed NPC growth through promoting cell apoptosis. However, we also found that ZNF750 knock down did not influence on cell apoptosis or cell growth apparently (Fig. 7h, i). Considering the low expression level of ZNF750 in NPC, we speculated that the gene did not function in normal NPC cells.

METTL3 modulated *ZNF750* expression epitranscriptionally and served as a prognostic factor in HNSC; therefore, we tested whether METTL3 was involved in NPC progression. Similar to ZNF750, cell cycle status did not change upon manipulating *METTL3* expression (Fig. 8a, b), while cell apoptosis was significantly activated when *METTL3* was knocked down, and vice versa (Fig. 8c, d). Concomitantly, colony formation assay and

cell growth analysis also illustrated that METTL3 functioned as an oncogene in NPC (Fig. 8e-h).

## Discussion

Until now, little was known about the effect of  $m^6A$  in NPC. DNA methylation in NPC has been examined in previous studies<sup>5,22-24</sup>. As an important supplement to the central dogma,  $m^6A$ -mediated RNA methylation and its role in cancer is only just beginning to be studied. Our work revealed that METTL3 mediated  $m^6A$  modification blocked ZNF750 expression and thus promoted NPC growth, which presented an example showing  $m^6A$  played essential regulatory roles post-transcriptionally in NPC. Considering that *ZNF750* is hypomethylated at its promoter and hypermethylated as mRNA, we hypothesize that epigenetic and epitranscriptional modifications may function together to modulate gene expression in some cases, complicating the study of the molecular mechanism governing NPC progression. Moreover, we identified *METTL3* as an



oncogene in NPC. In addition to ZNF750, we cannot exclude the involvement of other genes in NPC progression whose expression levels are affected by METTL3-mediated m<sup>6</sup>A modification. Therefore, similar to studies on DNA methylation, more research is required to reveal the whole m<sup>6</sup>A modification landscape in NPC.

ZNF750 was reported to be indispensable for terminal epidermal differentiation through regulating KLF4 expression<sup>25</sup>. A previous study also revealed that ZNF750

acted as a tumor repressor capable of promoting apoptosis through large-scale genomic analysis in 4742 samples spanning 21 tumor types<sup>17</sup>. However, the functional mechanism of ZNF750 in cancer remains obscure. Our findings identified *FGF14* as the direct target gene of ZNF750, and the ZNF750-FGF14 signaling axis inhibited NPC growth through promoting cell apoptosis, which broadened our understanding of ZNF750 in repressing tumor development.

FGF/FGFR signaling is involved in a variety of cellular processes, including tumorigenesis<sup>26,27</sup>. FGF14, as a member of the non-secreted type FGF family, does not function as an FGF ligand<sup>28</sup>. A previous study revealed that FGF14 regulates spinocerebellar development, the loss of which leads to spinocerebellar ataxia in mice<sup>29</sup>. However, there are no reports on FGF14 in cancer. Our findings revealed that FGF14 was repressed in NPC patients, and served as the direct target of ZNF750. Moreover, blocking cell apoptosis is one of the main characteristics of cancer. Targeting and promoting apoptotic processes is regarded as an effective method for anti-cancer therapy<sup>30–32</sup>. Our study demonstrated that the ZNF750-FGF14 signaling axis promoted tumor cell apoptosis, which may help to identify new therapeutic targets in NPC. However, the functional mechanism of FGF14 still needs to be explored in future studies.

## Conclusion

The m<sup>6</sup>A modification in ZNF750 facilitates its down-regulation in NPC, which promotes NPC progression. Overexpression of *ZNF750* blocked tumor cell growth in vitro and in vivo, while FGF14 functions as the downstream target of ZNF750 to regulate NPC apoptosis. These findings provide new insights into the molecular regulatory mechanism governing NPC progression, which may lead to new clinical treatment strategies in NPC.

## Materials and methods

### Ethical approval

This study was performed in accordance with ethical standards, according to the Declaration of Helsinki, and according to national and international guidelines. The study was approved by the ethics committee of Sun Yat-sen university Cancer center, and the approval number is YB2018-28.

### Patients and tumor tissue samples

Tumor samples were obtained from patients with pathologically confirmed NPC ( $n = 25$ ) at Sun Yat-sen University Cancer Center. No patients received clinical treatment before sampling, and all patients provided the written informed consent.

### Cell lines

NP69, a human immortalized nasopharyngeal epithelial (NPEC) cell line, was cultured in keratinocyte serum-free medium (Invitrogen, Life Technologies, Grand Island, NY) with bovine pituitary extract (BD, Biosciences, USA). NPC cell lines 5–8 F, 6–10B, C666-1, HNE1, HONE1, S18, S26, and SUNE1 were cultured in RPMI-1640 (Invitrogen) supplemented with 5% FBS (Gibco, Carlsbad, CA, USA). The cells were seeded in 6-well plates the day before transfection, which was performed using

Lipofectamine 3000 (Invitrogen), and the cells were harvested two days later.

### RNA extraction and reverse transcription-PCR (RT-PCR)

Total RNA from cell lines was extracted using the TRIzol reagent (Invitrogen). For the sorted cells from NPC biopsy samples, RNA was extracted using an RNeasy Micro kit (Qiagen, Hilden, Germany) following the manufacturer's instructions. cDNA was synthesized using M-MLV reverse transcriptase (Promega, Madison, WI, USA), and amplified using SYBR Green qRT-PCR SuperMix-UDG reagents (Invitrogen) and a CFX96 instrument (Bio-Rad, Hercules, CA, USA). The genes were amplified using the following primers: *GAPDH* forward, 5'-GAAGGTGAAGGTCGGAGT-3', and reverse 5'-GAAGATGGTGATGGGATTTC-3', *ZNF750* forward, 5'-TACAGCCCCAGGAACATC-3', and reverse 5'-GCTCCTTGCTGGGATTTT-3', *FGF14* forward, 5'-TATGAAAGGGAACAGAGTAAAG-3', and reverse 5'-CAGGACGAATAAGTCACAAC-3', *METTL3* forward, 5'-AGGGTCTGGATTGTGATG-3', and reverse 5'-CTGGGTCTAGTAGGTGGA-3'.

### ChIP-Seq

About  $1 \times 10^7$  SUNE1 cells with ZNF750-HA overexpression were harvested and treated according to the instructions of Pierce™ Magnetic ChIP kit (Thermo Fisher Scientific, Waltham, MA, USA). The cell extracts were collected and sent for sequencing by the Beijing Genomics Institute (BGI, Shenzhen, China). The qRT-PCR primers used for detecting *FGF14* in the ChIP assay were listed as follows: *FGF14* forward, 5'-CCACCCATCCTCATA GCG-3', and reverse 5'-AGCATGAAGCCAAACAGA-3'.

### Western blot and immunofluorescence

Total protein were extracted using RIPA lysis buffer (Beyotime, China). Proteins were separated by SDS-polyacrylamide gel electrophoresis (SDS-PAGE), and transferred onto PVDF membranes (Millipore, Billerica, MA, USA). The membranes were then incubated with primary antibodies against the HA tag (1:2000, H6908, Sigma-Aldrich, Munich, Germany), Flag tag (1:2000, F2555, Sigma), METTL3 (1:1000, ab195352, Abcam, Cambridge, MA, USA), or GAPDH (1:1000, ab8245, Abcam) at 4 °C overnight. After incubation with species-matched secondary antibodies, the immunoreactive proteins were detected using chemiluminescence in a Gel imaging system (Bio-Rad, ChemiDoc MP Imaging System). For immunofluorescence, cells overexpressing *ZNF750* were seeded and cultured on cover glass, and then fixed by methanol after 24 h of culture. The cells were then reacted with anti-HA antibody (1:500, H6908, Sigma), followed with the corresponding secondary

fluorescent antibody. The cells were viewed using confocal microscopy (Olympus, Tokyo, Japan).

#### Stable cell line establishment and shRNA treatment

The *ZNF750*, *FGF14*, and *METTL3* coding sequences were cloned into the pSin-EF2-puro vector, separately. The stably overexpressing cell lines were obtained by puromycin screening and confirmed by western blotting. Short hairpin RNA (shRNA) targeting *FGF14* or *METTL3* were designed using an online tool (GPP Web Portal), and cloned into vector pLKO. The shRNA target sequences of the *ZNF750*, *FGF14*, and *METTL3* were listed below: *ZNF750* target sequence, 5'-GAGTTCCCAAGTGCCCTAAAT-3', *FGF14* target sequence, 5'-ACCAGGTTATATTGCAGGCAA-3', *METTL3* target sequence, 5'-GC CAAGGAACAATCCATTGTT-3'.

#### Cell proliferation, colony formation assay, and cell invasion

The CCK-8 assay was used to detect cell proliferative ability.  $1 \times 10^3$  cells were seeded into 96-well plates, incubated for 0–4 days, and stained using the CCK-8 kit (Dojindo, Tokyo, Japan). The absorbance values were determined at 450 nm using a spectrophotometer. For the colony formation assay, about 300 cells were seeded into 6-well plates. After 7–10 days of culture, the cells were fixed by methanol and stained with crystal violet. For the cell invasion assay,  $3 \times 10^3$  cells were seeded into the 24-well Transwell chambers (Corning, NY, USA). The medium was supplemented with 10% FBS and placed in the lower chambers. After 14–18 h of culture, the chambers were collected and the cells on lower surface of the chambers were fixed by methanol and stained with crystal violet for observation.

#### EdU staining and cell apoptosis detection

For EdU staining,  $1 \times 10^5$  cells were seeded into 6-well plates. After the cell density reached about 90%, EdU (10  $\mu$ M, C0088S, Beyotime) was added, and the staining procedure was operated following the manufacturer's instructions. The cell cycle status were analyzed by flow cytometry (CytoFLEX 1, Beckman Coulter, Brea, CA, USA). For cell apoptosis analysis,  $1 \times 10^5$  cells were seeded into 6-well plates. Before the cell density reached about 90%, the cells were collected and stained with Annexin V and propidium iodide (PI) (C1062, Beyotime), and then analyzed by flow cytometry (CytoFLEX 1).

#### Luciferase reporter assay

The wild-type and mutated *FGF14* promoter (1000 base pairs upstream of transcription start site) were cloned into firefly luciferase-expressing vector psiCHECK™ (Promega). For the luciferase reporter assay, cells were cotransfected with *ZNF750* and *FGF14* wild-type or mutated promoter reporter vectors. The luciferase activity was

examined by a Dual-luciferase Reporter System (Promega) following the manufacturer's instructions.

#### RNA immunoprecipitation (RIP)

About  $1 \times 10^7$  NPC cells with *METTL3* knocked-down or overexpressed were harvested and manipulated as the instructions of the Magna RIP™ kit (Millipore). Anti-m<sup>6</sup>A antibody (10  $\mu$ g antibody for 5  $\mu$ g of mRNA, Synaptic Systems, 202003) was used, and the immunoprecipitated RNA extracts were reverse-transcribed and examined by qRT-PCR. The primers for *ZNF750* used in m<sup>6</sup>A-RIP-qRT-PCR were listed: forward 5'-TCCAGCAATATCCCTCTAAC-3', and reverse 5'-CCTCAGGAATTGGACTTTTCG-3'.

#### Animal experiments

BALB/c-nu mice (4–6 weeks old, female) were purchased from Charles River Laboratories (Beijing, China), and SUNE1-vector-luciferase or SUNE1-ZNF750-luciferase cells ( $1 \times 10^6$ ) were subcutaneously injected into the dorsal or ventral flank. Tumor cells were monitored 7–10 days later. Luciferin was diluted into 15 mg/ml using phosphate-buffered saline (PBS), and 100  $\mu$ l of the solution was intraperitoneally injected into each mouse. Five minutes later, the mice were anesthetized and observed using an animal imaging system (IVIS Lumina LT, PerkinElmer, Waltham, MA, USA). All animal research was performed in accordance with the detailed rules approved by the Animal Care and Use Ethnic Committee of Sun Yat-sen University Cancer Center and all efforts were made to minimize animal suffering.

#### Immunohistochemistry

For immunohistochemistry, xenograft tumors were fixed with paraformaldehyde and embedded in paraffin. The samples were sectioned and mounted on slides. The sectioned slides were incubated by anti-KI67 antibodies (1:500, ab15580, Abcam) at 4 °C overnight. Then the sections were incubated with biotinylated secondary antibody bound to a horseradishperoxidase complex. The antibody was visualized by adding 3,3-diaminobenzidine, and the sections were counterstained with hematoxylin.

#### Statistical analysis

Statistical analyses were performed using SPSS 17.0 (SPSS Inc., Chicago, IL, USA). All data shown are representative of at least three independent experiments, and values are expressed as the mean  $\pm$  SD. Differences between two groups were analyzed using the two-tailed unpaired Student's *t*-test;  $p < 0.05$  was considered significant. For the correlation analysis, Pearson analysis method was used. All data in our study have been recorded at Sun Yat-sen University Cancer Center for future reference (RDDB2018000415).

### Acknowledgements

This work was supported by grants from the Youth Science and Technology Innovation Talent of Guangdong TeZhi Plan (2017TQ04R754), Natural Science Foundation of Guangdong Province (2017A030310227, 2017A030312003), the open project of State Key Laboratory of Oncology in South China (HN2017-03), Health & Medical Collaborative Innovation Project of Guangzhou City, China (201803040003), Innovation Team Development Plan of the Ministry of Education (No. IRT\_17R110), Overseas Expertise Introduction Project for Discipline Innovation (111 Project, B14035), National Natural Science Foundation of China (81802920), the Natural Science Funding of Shenzhen (JCYJ20160422091914681).

### Authors' contributions:

P.P.Z., Q.P.H., and Y.L. carried out all the experiments, prepared the figures, and drafted the manuscript. Y.Q.L., X.W., M.Z.H., J.Z., X.Y.R., Y.Q.W., X.J.Y., and Q.M.H. participated in the data analysis and interpretation of results. P.P.Z., J.M., and N. L. conceived the study and participated in the data analysis. All authors read and approved the manuscript.

### Author details

<sup>1</sup>State Key Laboratory of Oncology in South China, Collaborative Innovation Centre of Cancer Medicine, Guangdong Key Laboratory of Nasopharyngeal Carcinoma Diagnosis and Therapy, Sun Yat-sen University Cancer Center, 510060 Guangzhou, China. <sup>2</sup>Zhongshan School of Medicine, Sun Yat-sen University, 510080 Guangzhou, China. <sup>3</sup>Guangdong Provincial Key Laboratory of Stomatology, Guanghua School of Stomatology, Sun Yat-sen University, 510055 Guangzhou, Guangdong, China

### Conflict of interest

The authors declare that they have no conflict of interest.

### Publisher's note

Springer Nature remains neutral with regard to jurisdictional claims in published maps and institutional affiliations.

**Supplementary Information** accompanies this paper at (<https://doi.org/10.1038/s41419-018-1224-3>).

Received: 10 May 2018 Revised: 9 November 2018 Accepted: 16 November 2018

Published online: 05 December 2018

### References

- Cao, S. M., Simons, M. J. & Qian, C. N. The prevalence and prevention of nasopharyngeal carcinoma in China. *Chin. J. Cancer* **30**, 114–119 (2011).
- McDermott, A. L., Dutt, S. N. & Watkinson, J. C. The aetiology of nasopharyngeal carcinoma. *Clin. Otolaryngol. Allied Sci.* **26**, 82–92 (2001).
- Wei, W. I. & Sham, J. S. Nasopharyngeal carcinoma. *Lancet* **365**, 2041–2054 (2005).
- Lai, S. Z. et al. How does intensity-modulated radiotherapy versus conventional two-dimensional radiotherapy influence the treatment results in nasopharyngeal carcinoma patients? *Int. J. Radiat. Oncol. Biol. Phys.* **80**, 661–668 (2011).
- Jiang, W. et al. Genome-wide identification of a methylation gene panel as a prognostic biomarker in nasopharyngeal carcinoma. *Mol. Cancer Ther.* **14**, 2864–2873 (2015).
- Yang, H. et al. Overexpression of tumor suppressor gene ZNF750 inhibits oral squamous cell carcinoma metastasis. *Oncol. Lett.* **14**, 5591–5596 (2017).
- Otsuka, R. et al. ZNF750 expression as a novel candidate biomarker of chemoradiosensitivity in esophageal squamous cell carcinoma. *Oncology* **93**, 197–203 (2017).
- Meyer, K. D. et al. Comprehensive analysis of mRNA methylation reveals enrichment in 3' UTRs and near stop codons. *Cell* **149**, 1635–1646 (2012).
- Dominissini, D. et al. Topology of the human and mouse m6A RNA methylomes revealed by m6A-seq. *Nature* **485**, 201–206 (2012).
- Perry, R. P., Kelley, D. E., Friderici, K. & Rottman, F. The methylated constituents of L cell messengerRNA: evidence for an unusual cluster at the 5' terminus. *Cell* **4**, 387–394 (1975).
- Bokar, J. A., Shambaugh, M. E., Polayes, D., Matera, A. G. & Rottman, F. M. Purification and cDNA cloning of the AdoMet-binding subunit of the human mRNA (N6-adenosine)-methyltransferase. *RNA (New York, N. Y.)* **3**, 1233–1247 (1997).
- Liu, J. et al. A METTL3-METTL14 complex mediates mammalian nuclear RNA N6-adenosine methylation. *Nat. Chem. Biol.* **10**, 93–95 (2014).
- Wang, X. et al. N6-methyladenosine-dependent regulation of messenger RNA stability. *Nature* **505**, 117–120 (2014).
- Schoenberg, D. R. & Maquat, L. E. Regulation of cytoplasmic mRNA decay. *Nat. Rev. Genet.* **13**, 246–259 (2012).
- Zhang, C. et al. Hypoxia induces the breast cancer stem cell phenotype by HIF-dependent and ALKBH5-mediated m(6)A-demethylation of NANOG mRNA. *Proc. Natl Acad. Sci. USA* **113**, E2047–E2056 (2016).
- Vu, L. P. et al. The N(6)-methyladenosine (m(6)A)-forming enzyme METTL3 controls myeloid differentiation of normal hematopoietic and leukemia cells. *Nat. Med.* **23**, 1369–1376 (2017).
- Lawrence, M. S. et al. Discovery and saturation analysis of cancer genes across 21 tumour types. *Nature* **505**, 495–501 (2014).
- Cancer Genome Atlas Network. Comprehensive genomic characterization of head and neck squamous cell carcinomas. *Nature* **517**, 576–582 (2015).
- Cancer Genome Atlas Network et al. Integrated genomic characterization of oesophageal carcinoma. *Nature* **541**, 169–175 (2017).
- Gao, J. et al. Integrative analysis of complex cancer genomics and clinical profiles using the cBioPortal. *Sci. Signal.* **6**, pii (2013).
- Cerami, E. et al. The cBio cancer genomics portal: an open platform for exploring multidimensional cancer genomics data. *Cancer Discov.* **2**, 401–404 (2012).
- Li, L. L., Shu, X. S., Wang, Z. H., Cao, Y. & Tao, Q. Epigenetic disruption of cell signaling in nasopharyngeal carcinoma. *Chin. J. Cancer* **30**, 231–239 (2011).
- Kwong, J. et al. Promoter hypermethylation of multiple genes in nasopharyngeal carcinoma. *Clin. Cancer Res.* **8**, 131–137 (2002).
- Zhang, J. et al. Epigenetic mediated zinc finger protein 671 downregulation promotes cell proliferation and tumorigenicity in nasopharyngeal carcinoma by inhibiting cell cycle arrest. *J. Exp. Clin. Cancer Res.* **36**, 147 (2017).
- Sen, G. L. et al. ZNF750 is a p63 target gene that induces KLF4 to drive terminal epidermal differentiation. *Dev. Cell* **22**, 669–677 (2012).
- Eswarakumar, V. P., Lax, I. & Schlessinger, J. Cellular signaling by fibroblast growth factor receptors. *Cytokine Growth Factor Rev.* **16**, 139–149 (2005).
- Katoh, M. & Nakagama, H. FGF receptors: cancer biology and therapeutics. *Med. Res. Rev.* **34**, 280–300 (2014).
- Smallwood, P. M. et al. Fibroblast growth factor (FGF) homologous factors: new members of the FGF family implicated in nervous system development. *Proc. Natl Acad. Sci. USA* **93**, 9850–9857 (1996).
- Wozniak, D. F., Xiao, M., Xu, L., Yamada, K. A. & Ornitz, D. M. Impaired spatial learning and defective theta burst induced LTP in mice lacking fibroblast growth factor 14. *Neurobiol. Dis.* **26**, 14–26 (2007).
- Chen, Y. M., Chen, P. L., Arnaiz, N., Goodrich, D. & Lee, W. H. Expression of wild-type p53 in human A673 cells suppresses tumorigenicity but not growth rate. *Oncogene* **6**, 1799–1805 (1991).
- Miyashita, T. & Reed, J. C. Tumor suppressor p53 is a direct transcriptional activator of the human bax gene. *Cell* **80**, 293–299 (1995).
- Oltersdorf, T. et al. An inhibitor of Bcl-2 family proteins induces regression of solid tumours. *Nature* **435**, 677–681 (2005).